Fantidis et al. Journal of Theoretical and Applied Physics 2012, 6:20
http://www.jtaphys.com/content/6/1/20

Journal of Theoretical and Applied Physics
a SpringerOpen Journal

RESEARCH **Open Access**

# Fast and thermal neutron radiographies based on a compact neutron generator

Jacob G Fantidis*, Bandekas V Dimitrios, Potolias Constantinos and Vordos Nick

**Abstract**

Fast neutrons that are produced via compact neutron generators have been used for thermal and fast neutron radiographies. In order to investigate objects with different sizes and produce radiographs of variable qualities, the proposed facility has been considered with a wide range of values for the parameters characterizing the thermal and fast neutron radiographies. The proposed system is designed according to article 4 of the Restriction of Hazardous Substances Directive 2002/95/EC, hence, excluded the use of cadmium and lead, and has been simulated using the MCNP4B code. The Monte Carlo calculations were carried out using three different neutron sources: deuterium-deuterium, deuterium-tritium, and tritium-tritium neutron generators.

**Keywords :** Fast neutron radiography, Thermal neutron radiography, Restriction of hazardous substances directive, Compact neutron generator, MCNP4B

**PACs: 28.20.Pr, 21.60.Ka, 24.10.Lx, 29.25.Dz.**

## Background

Neutron radiography (NR) has been around since the first research reactors became available in the 1950s and has grown in use and application throughout that time. NR is a technique of growing importance to science and industry, particularly as a method of nondestructive testing [1]. The technique is commonly used in security applications, engineering studies, geology, medicine, and biological research [2-5]. Depending on the neutron energy used, NR can be generally categorized as fast neutron radiography and thermal neutron radiography.

Due to the increasing availability of intense and brilliant thermal neutron beams at nuclear research reactors and neutron sources in recent years, the thermal NR became a well-accepted inspection technique. The fast NR is especially more suitable than the conventional thermal NR when the inspected object is thick or dense. This occurs due to the extremely high penetration depth of the fast neutrons in comparison with the thermal or cold neutrons in most materials of industrial interest [6,7]. A neutron radiography system mainly consists of the following three components: a neutron source, a collimator guiding the neutrons to the investigated object, and the detector placed behind the object (Figure 1).

The use of a deuterium-deuterium (DD) neutron generator for radiographic purposes has already been demonstrated by Fantidis et al. [8]. In this paper the proposed facility has been optimized for different neutron generators such as DD, deuterium-tritium (DT), and tritium-tritium (TT) using the MCNP4B Monte Carlo code [9]. The aim of the work was to design a unit which is suitable both for fast and thermal NR. The proposed system is designed according to article 4 of the European Union Restriction of Hazardous Substances Directive 2002/95/EC regarding the choice of materials [10]. Hence, lead, cadmium, mercury, hexavalent chromium, polybrominated biphenyls, and polybrominated diphenyl ethers have been excluded [11].

## Modeling

### *The neutron source*

There are a number of candidate neutron sources which are available for fast and thermal neutron radiography studies. The neutron generators have a compact size and offer an on/off switching of the emitted neutrons. They

* Correspondence: fantidis@yahoo.gr
Department of Electrical Engineering, Kavala Institute of Technology, St. Lucas, Kavala 65404, Greece

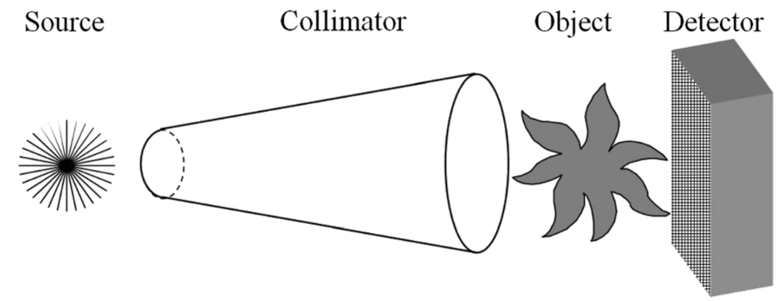


**Figure 1** Principle of neutron radiography.

can produce high neutron flux with logical cost, while the spectrum of the emitted neutrons extends up to 15.5 MeV (in a DT mode) [12]. The nuclear reactors and large accelerators, even though can generate neutron beams with high intensities, are extremely expensive permanent facilities. Isotropic neutron sources, such as $^{241}$Am/Be and $^{252}$Cf, although portable and relatively inexpensive, have low neutron intensity and they are not on/off switchable without special shutter systems (e.g.,$^{252}$Cf source) [8].

In this work, three neutron generators (DD, TT, and DT) were simulated based on a coaxial RF plasma neutron generator developed in Lawrence Berkeley National Laboratory (Berkeley, CA, USA) and by Adelphi Technology Inc (Redwood City, CA, USA). Neutrons in these generators are formed by using D-D, T-T, or D-T fusion reaction. The deuterium, tritium or deuterium-tritium gas mixture is ionized in an RF-driven plasma source. The ion beams are accelerated to approximately 120 keV energy using high current (350 mA) and high voltage DC power supply (120 kV), neutrons are produced when the beams impinge on a titanium target [13-15]. The facility has overall dimensions of $60 \times 45$ cm, with an extraction aperture composed of seven slits 1.5 mm wide and 75 mm in height [13]. The emitted neutron yield according to the manufacturer's guidelines is shown in Figure 2. The Figure 2 shows the normalized neutron spectra for each mode. The total neutron fluxes are $10^{11}$ ns$^{-1}$ for DD and TT mode and $10^{13}$ ns in the case of DT neutron generator [16-19].

### *Fast neutron collimator*

The quality of fast NR imaging is determined by the collimator ratio ($L/D$) where $L$ is the length of the collimator and $D$ is the collimator aperture diameter. The geometric unsharpness $u_g$, caused by the finite size of neutron source, is given by the equation [20]

$$u_g = \frac{DL_f}{L_\alpha - L_f} \tag{1}$$

where $L_f$ is the image surface to object distance and $L_a$ is the distance from the aperture to the image plane.

The beam quality profile determined by the number of uncollided neutrons that reach the detector position within the neutron beam could also characterize the imaging quality of a fast NR facility. Although no materials exist that would be strong absorbers for fast neutrons, suitable imaging systems can be effectively built and used. Metals are found to be more suitable as collimator material for fast neutrons. Then neutrons would be scattered away from the interior walls of a collimator following very few collisions, with an insignificant loss in energy. Hence, iron and tungsten are preferred as collimator materials. The low cost of iron (Fe) compared with tungsten and the difficulties associated with tungsten fabrication makes the former the best solution [21].

The geometrical configuration of the collimator for both fast and thermal NR used in the present study is similar to the one described previously, in [8], with a minor difference in geometry. Figure 3 shows the proposed collimator system for fast NR. In keeping with

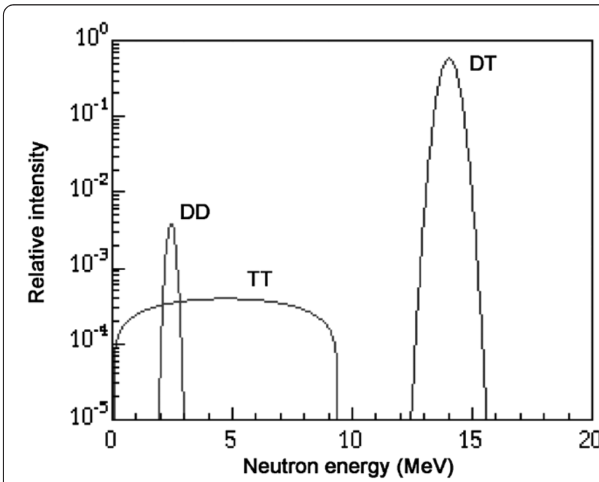


**Figure 2** Normalized neutron spectra for DD, TT, and DT neutron generator.

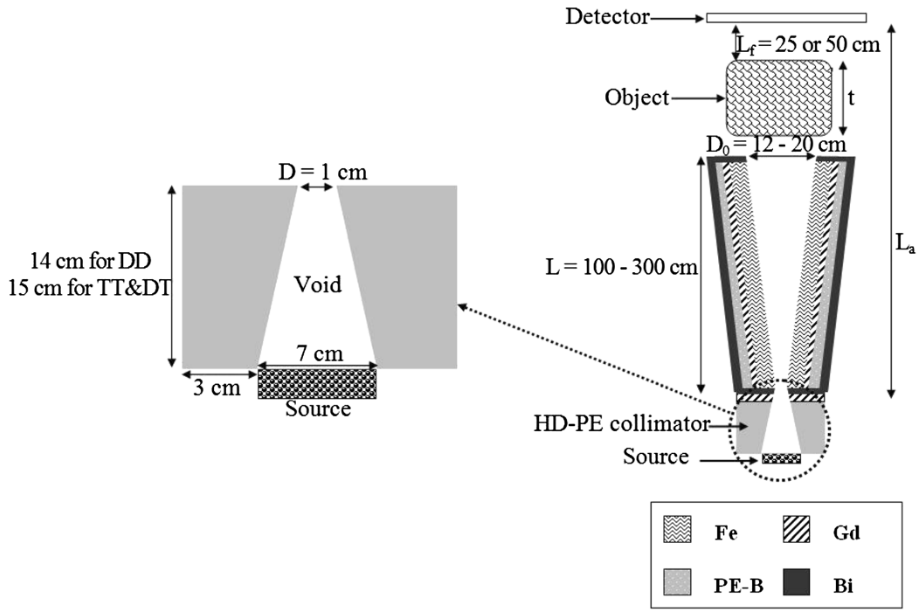


**Figure 3** The aperture geometry and the collimator for fast neutron radiography (not in scale).

Figure 3, the fast neutron collimator studied in this work comprises two parts. The first, which is a high-density polyethylene cylinder with a radius of 10 cm, incorporates a void conic convergent collimator, with length of 14 cm for DD source and 15 cm for DT and TT neutron sources. The convergent collimator has radii of 3.75 and 0.5 cm, with the larger radius close to the source.

The second collimator, which is a divergent one with an inlet aperture of 1 cm and changeable length and walls, is made of four layers of different materials. These materials (from the inside outwards) are 8-cm thick iron (Fe), 0.5-cm thick gadolinium (Gd), 2-cm thick polyethylene with 5% boron (PE-B), and 1.5-cm bismuth (Bi). Between the two collimators is an aperture consisting of two materials: 0.3 and 1 cm thick layers of Gd and Bi, respectively, which are used to absorb thermal neutrons whereas preventing the gamma rays originated within the other materials to reach the second collimator. Moreover, there is a 2-cm thick layer of Bi casing the front side of the collimator in order to provide a shield against any gamma rays that may be produced within the collimator's material by neutron activation. The recordings of the scattered neutrons, which affect the imaging contrast, depend on the object-to-detector distance ($L_f$) and reduce by $1/L_f^2$. When this distance increases, the scattered neutron intensity decreases by $1/L_f^2$, while the source neutron intensity in the detector plane decreases owing to the simultaneously increasing distance from aperture to the image plane.

#### *Thermal neutron collimator*

In a similar way as in the case of fast NR, the collimator ratio (*L/D*) determines the quality of the NR imaging for a given design. This ratio is described by the equations [22]:

$$\phi_i = \frac{\phi_\alpha}{16\left(\frac{L_S}{D}\right)^2} \tag{2}$$

and

$$u_g = L_f \frac{D}{L_s} \tag{3}$$

where $L_f$ is the image surface to object distance, $L_s$ is the source to object distance, $D$ is the inlet aperture diameter, $\phi_i$ is the neutron flux at the image plane, $\phi_\alpha$ is the neutron flux at the aperture and $u_g$ is the geometric unsharpness.

The spatial resolution of an image depends not only on the detector resolution but also strongly on the beam divergence. In addition, the quality of an image (spatial resolution) depends also on the beam divergence. The beam divergence is described by its half-angle ($\theta$) which is given by equation [22]

$$\theta = \tan^{-1}\left(\frac{I}{2L}\right) \tag{4}$$

where $I$ and $L$ are the maximum dimensions of the image area and the length of the collimator. The imaging quality of a system would be additionally characterized by the thermal neutron content (TNC), describing the number of thermal neutrons within the neutron beam

$$TNC = \frac{thermal\ neutron\ flux}{total\ neutron\ flux} \quad (5)$$

and the relative intensities of the neutron ($n$) and the photon ($\gamma$) components of the beam, with the ($n/\gamma$) typically greater than $10^4$ n cm$^{-2}$ mSv$^{-1}$ [23].

Since the neutron generators emit fast neutrons, in the case of thermal NR, the first step in the design of the unit is to slow down these fast neutrons to a lower temperature. The slowing down or thermalization is normally done with suitable moderating materials. HD-PE (in Equation 1) was used as a moderator in order to provide the maximum neutron flux at the collimator inlet aperture from the generators using layers with depths of 2.1, 2.4, and 2.8 cm for DD, TT, and DT sources, respectively (Figure 4).

The collimator is a combination of two parts. The first attached to the HD-PE moderator is an HD-PE cylinder, with a radius of 8 cm and length of 14 cm for DD generator or 15 cm for DT and TT neutron generators, and incorporated with a conic collimator made of either single sapphire ($Al_2O_3$) or void. The conic collimator has radii 3.75 and 1 cm, with the larger radius nearer to the source. The single sapphire is used for filtering out the fast neutrons from the collimated beam. High-quality single-sapphire crystals is better fast neutron filter than silicon or quartz [24], and the transmission properties of sapphire are not distorted by irradiation even after years within the neutron beam tube of a nuclear reactor [25].

The second part adjacent to the HD-PE cylinder is a divergent collimator, which is the basic component in neutron imaging and determines the quality of the image. The most important element of each collimator is its lining which should be made of a neutron-absorbing material [22]. The lining is composed of a 0.8-cm layer of boron covered by PE-B with a depth of 3.2 cm as a shield against stray neutrons. Bi with 1 cm thickness was chosen as the collimator casing.

## Results and discussion

### Penetration calculations

In order to evaluate the penetration of the neutron generators, five neutron sources (DD, TT, DT, $^{252}$Cf, and $^{241}$Am/Be) and one gamma source ($^{60}$Co) have been utilized. The results, which were obtained from the MCNP4B simulations, are shown in Figure 5. The penetration was determined using the F5 tally card which gives the neutron flux at a point in neutrons per square centimeters per starting neutron (Figure 5). This figure illustrates the thicknesses of various materials through which 0.1% of the neutrons are transmitted from DD, TT, or DT sources. According to the results, the DD neutron generator is significantly more penetrating for heavier elements and less penetrating for organic materials compared to a $^{60}$Co gamma source. The penetration of the TT source is larger than DD source and similar with $^{241}$Am/Be. As can be seen from the Figure 5, the DT neutron generator has the advantage of better penetration than all the other neutrons sources.

### Fast NR results

In the case of fast NR, the proposed system has been considered with a second collimator having variable

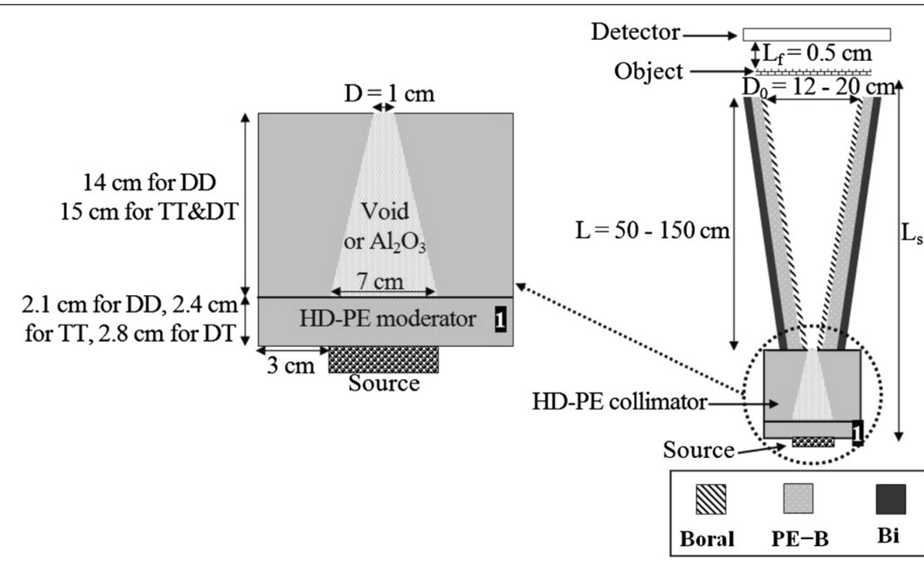


**Figure 4 The aperture geometry and the collimator for thermal neutron radiography (not in scale).**

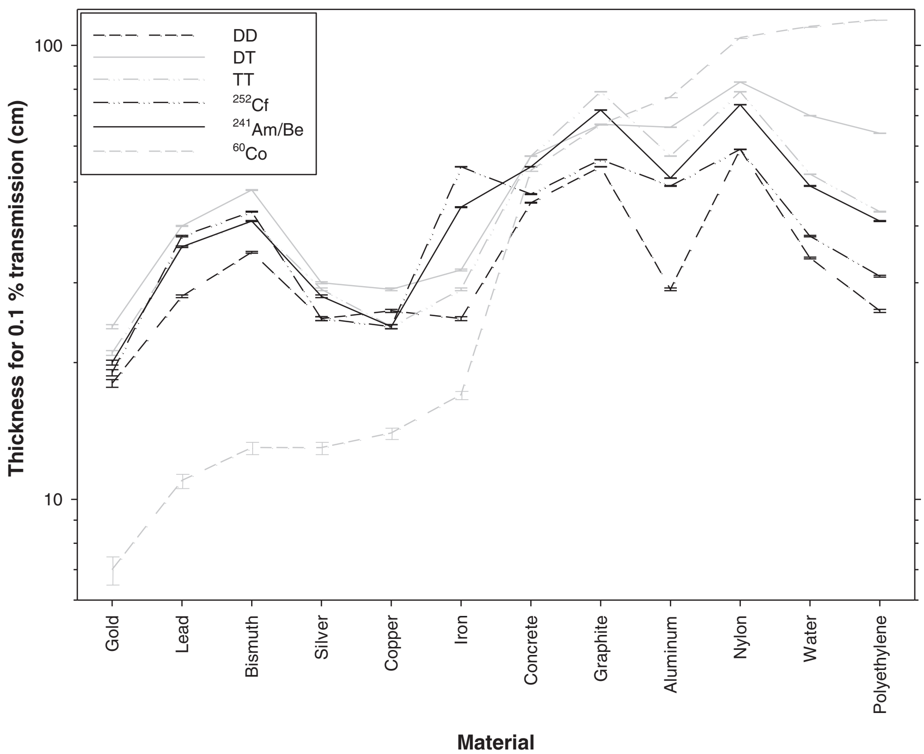


**Figure 5 Comparison of penetration for five neutron sources (DD, TT, DT,$^{252}$Cf and $^{241}$Am/Be) and one gamma source ($^{60}$Co).**

length ($L = 100$ to 300 cm) and diameter of its aperture next to the image plane ($D_0 = 12$ to 20 cm). The object-detector distance ($L_f$) was considered to be 25 or 50 cm. In order to calculate the $u_g$, it is necessary to know the object depth ($t$). In our simulations the $t$ was equal to $L_f$, so the distance between the end of the collimator and the detector was $2L_f$. In all circumstances, the $n/\gamma$ ratio has values that are about four orders in magnitude less than the recommended values.

Fast neutron fluxes ($f_F$) were calculated using the F2 tally which gives the required neutron flux an average over a surface in neutrons cm$^{-2}$ per starting neutron for the number of particle histories (NPS = $6 \times 10^7$) neutrons, yielding an accuracy <0.5%. The photon dose ($\gamma$) was calculated with the MCNP4B Monte Carlo code, using the F2, and Fm2 tallies combined with the DE and DF cards. The tallies describe the neutron flux over a surface, while the D cards convert the absorbed dose to equivalent dose. Calculations were performed for a total number of histories of $6 \times 10^6$, yielding an accuracy in the calculations of <1%.

The calculated parameters for the fast NR system are shown in Tables 1 and 2. In the case of DD neutron source, the uncollided fast neutron flux (uncollided $f_F$), which characterizes the beam quality [26], ranges between 97.09 to 98.55% for $L_f = 25$ cm and 97.28% to 98.76% for $L_f = 50$ cm. The total fast neutron flux ($f_F$) varies from $7.25 \times 10^3$ to $5.78 \times 10^4$ n cm$^{-2}$ s$^{-1}$. The $f_F$ at the field of view of the object was uniform to 1.5%. The good-quality fast neutron images require exposures in the order of $1.5 \times 10^7$ n cm$^{-2}$ [27], with the exposure time being analogous to the fast neutron flux. In the case of $L/D = 100$, the exposure time is 4.3 and 7.6 min at $L_f = 25$ cm and $L_f = 50$ cm distances, respectively.

**Table 1 The fast NR-calculated parameters using the proposal system with $t$ and $L_f = 25$ cm**

| $L/D$ | $D_0$ (cm) | $u_g$ (cm) | DD | | TT | | DT | |
|---|---|---|---|---|---|---|---|---|
| | | | Uncollided $f_F$ (%) | $f_F$ (n cm$^{-2}$ s$^{-1}$) | Uncollided $f_F$ (%) | $f_F$ (n cm$^{-2}$ s$^{-1}$) | Uncollided $f_F$ (%) | $f_F$ (n cm$^{-2}$ s$^{-1}$) |
| 100 | 12 | 2.00e-1 | 97.09 | 5.78e + 4 | 95.19 | 5.86e + 4 | 92.40 | 6.71e + 6 |
| 150 | 14 | 1.42e-1 | 97.75 | 3.18e + 4 | 96.38 | 3.12e + 4 | 95.36 | 3.45e + 6 |
| 200 | 16 | 1.11e-1 | 97.93 | 1.94e + 4 | 96.76 | 1.94e + 4 | 95.92 | 2.13e + 6 |
| 250 | 18 | 9.09e-2 | 98.27 | 1.31e + 4 | 97.36 | 1.32e + 4 | 96.54 | 1.44e + 6 |
| 300 | 20 | 7.69e-2 | 98.55 | 9.57e + 3 | 97.38 | 9.59e + 3 | 96.95 | 1.04e + 6 |

**Table 2 The fast NR-calculated parameters using the proposal system with $t$ and $L_f = 50$ cm**

| L/D | $D_0$ (cm) | $u_g$ (cm) | DD | | TT | | DT | |
|---|---|---|---|---|---|---|---|---|
| | | | Uncollided $f_F$ (%) | $f_F$ (n cm$^{-2}$ s$^{-1}$) | Uncollided $f_F$ (%) | $f_F$ (n cm$^{-2}$ s$^{-1}$) | Uncollided $f_F$ (%) | $f_F$ (n cm$^{-2}$ s$^{-1}$) |
| 100 | 12 | 3.33e-1 | 97.28 | 3.30e + 4 | 95.87 | 3.32e + 4 | 92.88 | 2.81e + 6 |
| 150 | 14 | 2.50e-1 | 97.98 | 2.01e + 4 | 96.68 | 2.01e + 4 | 95.89 | 2.21e + 6 |
| 200 | 16 | 2.00e-1 | 98.14 | 1.34e + 4 | 96.98 | 1.35e + 4 | 96.15 | 1.48e + 6 |
| 250 | 18 | 1.66e-1 | 98.47 | 9.72e + 3 | 97.51 | 9.71e + 3 | 96.66 | 1.06e + 6 |
| 300 | 20 | 1.42e-1 | 98.76 | 7.25e + 3 | 97.56 | 7.34e + 3 | 97.03 | 7.94e + 5 |

Higher $L/D$ values would require higher exposure times; for example, $L/D = 300$, which necessitates exposure times in the range of 26.1 to 34.4 min, gives radiographies a better quality. TT neutron generator has slightly worse results compared to the DD source. The $f_F$ varies from $7.34 \times 10^3$ to $5.86 \times 10^4$ n cm$^{-2}$ s$^{-1}$, while the uncollided $f_F$ ranges from 95.19 to 97.38% for $L_f = 25$ cm and between 95.87% and 97.56% for $L_f = 50$ cm.

In the case of DT neutron generator, the uncollided $f_F$ fluctuates between 92.40% and 96.95% for $L_f = 25$ cm and 92.88% to 97.03% for $L_f = 50$ cm. The $f_F$ varies from $7.94 \times 10^5$ to $6.71 \times 10^6$ n cm$^{-2}$ s$^{-1}$. Qualitative fast neutron images need exposures in the order of $1.8 \times 10^7$ n cm$^{-2}$ [28]. The high yield of DT coaxial neutron generator is able to offer radiographies in a very short time. For $L/D = 100$, the exposure time is 2.7 and 6.4 s with $L_f = 25$ and $L_f = 50$ cm, respectively; in the cases of $L/D =$ 200 and 300, exposure times are in the range of 8.45 to 12.2 s and 17.4 to 22.7 s. According to the values for the exposure time, the DT neutron generator is capable of producing real-time NR.

### Thermal NR results

The suggested system was further simulated for thermal NR. The divergent collimator has changeable length ($L = 50$ to 150 cm), diameter of its aperture next to the image plane ($D_0 = 12$ to 20 cm), and divergence angle ($\theta$) of the beam ($\theta = 1.4°$ to 5.7°); while the inlet aperture ($D$) of the collimator is 1 cm. The distance between the object and the imaging detector ($L_f$) was considered at 0.5 cm [22]. The variation of the thermal neutron flux at the field of view at the object position was less than 2%. The calculated thermal neutron flux ($f_{th}$), TNC, and ($n/\gamma$) parameters are given in Table 3 for different collimator parameters. The neutron flux was calculated with the aid of the MCNP4B code using the F2 tally, which gives the required neutron flux average over a surface in neutrons square centimeters per starting neutron. The calculations were carried out with NPS $= 6 \times 10^7$ neutrons, yielding an accuracy <0.5%. An energy boundary of 0.01 to 0.3 eV was used to score the thermal neutron flux. The dose rate due to the photons, ($\gamma$), was calculated with the MCNP4B Monte Carlo code using the F2, Fm2 tallies, and the DE and DF cards. Cutoff (NPS) values up to $3 \times 10^7$ histories were considered to yield an accuracy of <2% in the calculations.

The DT neutron generator gives the maximum values for the $f_{th}$ which varies from $4.03 \times 10^4$ to $3.81 \times 10^5$ n cm$^{-2}$ s$^{-1}$. On the occasion of DD and TT sources, the $f_{th}$ fluctuates among the values of $1.8 \times 10^3$ to $1.59 \times 10^4$ and $1.14 \times 10^3$ to $8.83 \times 10^3$ n cm$^{-2}$ s$^{-1}$, respectively. These values, especially in the case of DT neutron source, are comparable with fluxes from low power research reactors [29,30]. The ($n/\gamma$) parameter remains in all circumstances at least 70 times higher than the recommended limit of $10^4$ n cm$^{-2}$ mSv$^{-1}$. Due to the fact that the neutron generators emit mostly fast neutrons, the TNC cannot overcome the 0.53%, 2.26%, and 3.89% for DT, TT, and DD generators correspondingly (Table 3).

Except from the TNC, all the other parameters have values which forebode qualitative neutron radiographs. In order to optimize the TNC of the beam, sapphire is used as a fast neutron filter. For this reason the $f_{th}$, TNC, and ($n/\gamma$) parameters were determined for different sapphire filter thicknesses in the case of two $L/D$ values (Table 4). The $f_{th}$ has decreased up to 41.5%

**Table 3 Thermal NR-calculated parameters using the proposal unit**

| L/D | $D_0$ (cm) | $u_g$ (cm) | $\theta$ (°) | DD | | | TT | | | DT | | |
|---|---|---|---|---|---|---|---|---|---|---|---|---|
| | | | | $f_{th}$ (n cm$^{-2}$ s$^{-1}$) | $n/\gamma$ (n cm$^{-2}$ mSv$^{-1}$) | TNC (%) | $f_{th}$ (n cm$^{-2}$ s$^{-1}$) | $n/\gamma$ (n cm$^{-2}$ mSv$^{-1}$) | TNC (%) | $f_{th}$ (n cm$^{-2}$ s$^{-1}$) | $n/\gamma$ (n cm$^{-2}$ mSv$^{-1}$) | TNC (%) |
| 50 | 12 | 1.00e-2 | 6.8 | 1.59e + 4 | 7.03e + 5 | 3.58 | 8.83e + 3 | 4.38E + 7 | 2.02 | 3.81e + 5 | 7.25e + 7 | 0.46 |
| 75 | 14 | 6.67e-3 | 5.3 | 7.21e + 3 | 8.74e + 5 | 3.76 | 4.31e + 3 | 5.55E + 7 | 2.10 | 1.58e + 5 | 7.31e + 7 | 0.46 |
| 100 | 16 | 5.00e-3 | 4.6 | 4.11e + 3 | 9.11e + 5 | 3.88 | 2.36e + 3 | 6.44E + 7 | 2.11 | 8.99e + 4 | 7.29e + 7 | 0.49 |
| 125 | 18 | 4.00e-3 | 4.1 | 2.63e + 3 | 1.22e + 6 | 3.88 | 1.63e + 3 | 6.49E + 7 | 2.23 | 5.81e + 4 | 8.25e + 7 | 0.51 |
| 150 | 20 | 3.33e-3 | 3.8 | 1.82e + 3 | 1.31e + 6 | 3.89 | 1.14e + 3 | 6.67E + 7 | 2.26 | 4.03e + 4 | 8.36e + 7 | 0.53 |

**Table 4 Thermal NR-calculated parameters for minimum and the maximum L/D values with single sapphire filter**

| Sapphire filter (cm) | *L/D* = 50 | | | | | | *L/D* = 150 | | | | | |
|---|---|---|---|---|---|---|---|---|---|---|---|---|
| | DD | | TT | | DT | | DD | | TT | | DT | |
| | $f_{th}$ (n cm$^{-2}$ s$^{-1}$) | TNC (%) | $f_{th}$ (n cm$^{-2}$ s$^{-1}$) | TNC (%) | $f_{th}$ (n cm$^{-2}$ s$^{-1}$) | TNC (%) | $f_{th}$ (n cm$^{-2}$ s$^{-1}$) | TNC (%) | $f_{th}$ (n cm$^{-2}$ s$^{-1}$) | TNC (%) | $f_{th}$ (n cm$^{-2}$ s$^{-1}$) | TNC (%) |
| 0 | 1.59e + 4 | 3.58 | 8.83e + 3 | 2.02 | 3.81e + 5 | 0.46 | 1.82e + 3 | 3.89 | 1.14e + 3 | 2.26 | 4.03e + 4 | 0.53 |
| 5 | 1.28e + 4 | 7.86 | 7.28e + 3 | 3.64 | 3.14e + 5 | 0.79 | 1.49e + 3 | 9.36 | 9.39e + 2 | 4.37 | 3.31e + 4 | 0.96 |
| 10 | 1.09e + 4 | 18.45 | 6.16e + 3 | 6.40 | 2.66e + 5 | 1.38 | 1.27e + 3 | 21.36 | 7.96e + 2 | 8.43 | 2.79e + 4 | 1.56 |
| 14 (DD) or 15 (DT and TT) | 9.64e + 3 | 27.03 | 5.17e + 3 | 8.38 | 2.23e + 5 | 1.83 | 1.12e + 3 | 35.36 | 6.68e + 2 | 13.13 | 2.36e + 4 | 2.92 |

approximately, and the (*n/γ*) is still at least six times higher than the recommended limit.

The TNC has a considerable gain. In the case of DD generator, the TNC reaches 27.03% (3.58% without filter) or 35.36% (3.89% without filter) for *L/D* equal to 50 and 150, respectively. The improvement for TT neutron generator is also appreciable but smaller than the DD source. The TNC values vary between of 2.02% to 8.38% or 2.26% to 13.13% for *L/D* = 50 and *L/D* = 150 correspondingly. Finally, in the case of DT generator, although there is a noticeable difference, the fast neutron content in the beam is significant. With the purpose to detect defects lower than 0.025 cm, the thermal NR requires exposures in the order of $10^7$ n cm$^{-2}$ [31], and Table 5 show the exposure time in each case.

## Conclusions

The fast and thermal neutron radiography facilities have been simulated using the MCNP4B Monte Carlo code. Suitable collimators have been simulated for the two radiography options. All the selected materials were chosen according to the European Union Directive 2002/95/EC, hence, excluded lead and cadmium. The results of the simulation study showed that neutron generators are suitable for both thermal and fast neutron radiography studies and have similar performance. In the case of thermal NR, the DD source is able to offer radiographs with slightly better quality than TT or DT neutron generator, but the DT source with the higher neutron output is able to reduce the exposure time. For fast NR the DD and TT sources have similar results, but the TT has better penetration through the materials. The DT neutron generator owing to its neutrons, with higher flux and energy, seems to be the best solution.

**Table 5 The required time for quality thermal NR**

| Sapphire filter (cm) | *t* (min) | | | | | |
|---|---|---|---|---|---|---|
| | *L/D* = 50 | | | *L/D* = 150 | | |
| | DD | TT | DT | DD | TT | DT |
| 0 | 10.48 | 18.88 | 0.44 | 91.58 | 146.20 | 4.14 |
| 5 | 13.02 | 22.89 | 0.53 | 111.86 | 177.49 | 5.04 |
| 10 | 15.29 | 27.06 | 0.63 | 131.23 | 209.38 | 5.97 |
| 14 (DD) or 15 (DT and TT) | 17.29 | 32.24 | 0.75 | 148.81 | 249.50 | 7.06 |

## Methods

Based on the use of three different types of neutron generators, namely DD, DT, and TT, a unit has been simulated, both for fast and thermal radiography purposes, using the MCNP4B Monte Carlo code. Appropriate collimators have been designed for each of the radiography modes with small alteration in the dimensions of the unit which are dependents of the neutron spectrum of the generator. All the materials considered were chosen according to the European Union Directive 2002/95/EC, excluding lead and cadmium. The proposed facilities have been simulated for a wide range of values for the parameters characterizing the thermal and fast neutron radiographies. In the case of Fast NR, simulations were carried out at five different values of the collimator ratio (*L/D*) 100, 150, 200, 250, and 300. The object-detector distance (*t*) was considered to be 25 or 50 cm. In the case of thermal NR, simulations were performed for collimator ratio equal to 50, 75, 100, 125, and 150. The proposed system was further simulated for minimum and maximum values of the collimator ratio for different sapphire filter thicknesses which is commonly used for fast neutron filtration.

### Competing interests

The authors declare that they have no competing interests.

### Authors' contributions

JGF designed the geometry and carried out the simulations with MCNP4B. DVB participated in the simulations with MCNP4B. CP and VN participated in the design of the geometry. All authors read and approved the final manuscript.

### Authors' information

JGF is a scientific assistant at the Kavala Institute of Technology. DVB holds the position as professor in the Department of Electrical Engineering at the Kavala Institute of Technology. CP is a lecturer from the Department of Electrical Engineering at the Kavala Institute of Technology. VN is a laboratory assistant in the Department of Electrical Engineering at the Kavala Institute of Technology.

**Acknowledgments**
The authors gratefully acknowledge Prof. Hadi Savaloni, member of the *Journal of Theoretical and Applied Physics* editorial team and the anonymous reviewers for their valuable contributions.

Received: 21 April 2012 Accepted: 26 August 2012
Published: 4 September 2012

## References

1. Strobl, M, Kardjilov, N, Hilger, A, Dawson, M, Banhart, J: Advances in neutron radiography and tomography. Journal of Physics D **42**, 21 (2009)
2. Wang, X, Wong, BS, Tan, C, Tui, CG: Automated crack detection for digital radiography aircraft wing inspection. Res. Nondestruct. Eval. **22**, 105 (2011)
3. Middleton, MF, Pázsit, I, Solymar, M: Petrophysical applications of neutron radiography. Nondestr. Test. Eval. **16**, 321 (2001)
4. Nir-El, Y, Katz, V, Haddad, J, Eliezer, D: Determination of structure and composition in ceramics and aerospace materials by neutron radiography. Nondestr. Test. Eval. **11**, 149 (1994)
5. De-Beer, FC, Strydom, WJ: Neutron radiography at SAFARI-I in South Africa. Nondestr. Test. Eval. **16**(2), 163 (2001)
6. Bai, JH, Shin, M, Whang, JH, Monte Carlo, A: Calculation for neutron radiography facility using sealed-tube neutron generator, pp. 5–10. 12th A-PCNDT 2006 - Asia-Pacific Conference on NDT, Auckland, New Zealand (2006)
7. Mikerov, VI, Zhitnik, IA, Barmakov, JN, Zhitnik, IA, Barmakov, JN, Bogolubov, EP, Ryzhkov, VI, Koshelev, AP, Soshin, NP, Waschkowski, W, Lanza, RC, Hall, JM: Prospects for efficient detectors for fast neutron imaging. Appl. Radiat. Isot. **61**, 529 (2004)
8. Fantidis, JG, Nicolaou, GE, Tsagas, NF: Optimization study of a transportable neutron radiography unit based on a compact neutron generator. Nuclear Instruments and Methods in Physics Research A **618**, 331 (2010)
9. Briesmeister, JF: MCNP4B MCNP™ - A General Monte Carlo N-particle Transport Code, Version 4B LA-12625-M Manual. (2012). http://mightylib.mit.edu/Student%20Materials/books/mcnp4b.pdf (1997). Accessed 29 August 2012
10. Euopean Union: Official Journal of the European Union, L37/19, 13.2.2003. http://eur-lex.europa.eu/LexUriServ/LexUriServ.do?uri=OJ:L:2003:037:0019:0023:en:PDF (2003). Accessed 29 August 2012
11. Mellow, BD, Thomas, DJ, Joyce, MJ, Kolkowski, P, Roberts, JN, Monk, SD: The replacement of cadmium as a thermal neutron filter. Nuclear Instruments and Methods in Physics Research A **577**, 690 (2007)
12. Leung, K-N, Reijonen, J, Gicquel, F, Hahto, S, Lou, TP: Compact neutron generator development and applications. 16th World Conference on NDT, Montreal, Canada (2004). 30 August-3 September 2004
13. Reijonen, J, Gicquel, F, Hahto, SK, King, M, Lou, T-P, Leung, K-N: D-D neutron generator development at LBNL. Appl. Radiat. Isot. **63**, 757 (2005)
14. Reijonen, J, Leung, KN, Jones, G: RF ion source development for neutron generation and for material modification. Rev. Sci. Instrum. **73**, 934 (2002)
15. Reijonen, J: Neutron generators for detection of explosives and illicit materials, pp. 13–16. IAEA Technical Meeting on Neutron Generators, Vienna, Austria (2005)
16. Reijonen, J: Compact neutron generators for medical, home land security and planetary exploration, pp. 16–20. Knoxville, Tennessee, (2005). May 2005
17. Reijonen, J, Andresen, N, Gicquel, F, Gough, R, King, M, Kalvas, T, Leung, K-N, Lou, T-P, Vainionpa, H, Antolak, A, Morse, D, Doyle, B, Miller, G, Piestrup, M: Development of advanced neutron/gamma generators for imaging and active interrogation applications. Proceedings of SPIE **6540**, 65401P–65412P (2007)
18. Williams, DL, Vainionpaa, JH, Jones, G, Piestrup, MA, Gary, CK, Harris, JL, Fuller, MJ, Cremer, JT, BA, L, Kwan, JW, Reijonen, J, Leung, K-N, Gough, RA: High intensity, pulsed, D-D neutron generator. AIP Conf. Proc. **1099**, 936 (2008)
19. Christian, JF, Sia, R, Dokhale, P, Shestakova, I, Nagarkar, V, Shah, K, Johnson, EB, Stapels, CJ, Ryan, JM, Macri, J, Bravar, U, Leung, KN, Squillante, MR: Nuclear material detection techniques. MR: Proc. of SPIE Vol **6945**, 69451Q (2008)
20. Berger, H, Iddings, F: Neutron Radiography - a State-of-the-Art Report. Nondestructive Testing Information Analysis Center, NTIAC, Austin (1998)
21. Hussein, EM: Handbook on Radiation Probing, Gauging. Imaging and Analysis Volume II Applications and Design, Kluwer Academic Publishers, Dordrecht (2004)
22. Domanus, JC: Collimators for Thermal Neutron Radiography - an Overview. D. Reidel Publishing, Dordrecht (1987)
23. Hawkesworth, MR: Neutron radiography: equipment and methods. Atomic Energy. Review **15**, 169 (1977)
24. Tennant, DC: Performance of a cooled sapphire and beryllium assembly for filtering of thermal neutrons. Rev. Sci. Instrum. **59**(2), 380 (1988)
25. Mildner, DFR, Lamaze, GP: Neutron transmission of single-crystal sapphire. J Appl. Crystallogr. **31**, 835 (1998)
26. Bucherl, T, Kutlar, E, von Gostomski, CL, Calzada, E, Pfister, G, Koch, D: Radiography and tomography with fast neutrons at the FRM-II - a status report. Appl. Radiat. Isot. **61**, 537 (2004)
27. Mikerov, V, Waschkowski, W: Fast neutron fields imaging with a CCD-based luminescent detector. Nuclear Instruments and Methods in Physics Research A **424**, 48 (1999)
28. Sanami, T, Baba, M, Saito, K, Yamazaki, T, Miura, T, Ibara, Y, Taniguchi, S, Yamadera, A, Nakamura, T: Fast-neutron profiling with an imaging plate. Nuclear Instruments and Methods in Physics Research A **458**, 720 (2001)
29. Zawisky, M, Hameed, F, Dyrnjaja, E: Digitized neutron imaging with high spatial resolution at a low power research reactor: I. Analysis of detector performance. Nuclear Instruments and Methods in Physics Research A **587**(342) (2008)
30. Chankow, N, Punnachaiya, S, Wonglee, S: Neutron radiography using neutron imaging plate. Appl Radiat Isot **68**, 662 (2010)
31. Gibbs, KM, Berger, H, Jones, T, Polansky, D, Haskins, J, Schneberk, D, Brenizer, J: Flat panel imaging of thermal neutrons, p. 140. ASNT Fall Conference Summaries, Columbus (1999)

doi:10.1186/2251-7235-6-20
**Cite this article as:** Fantidis *et al.*: Fast and thermal neutron radiographies based on a compact neutron generator. *Journal of Theoretical and Applied Physics* 2012 **6**:20.